Electronic Supplementary Material (ESI) for Physical Chemistry Chemical Physics.

Electronic Supporting Information

Revealing the Electronic Character of the Positive Electrode/Electrolyte Interface in Lithium-Ion Batteries

G. Zampardi[a,b,c], R. Trocoli[b,c], W. Schuhmann†[c] and F. La Mantia†[b,e]

a. Department of Chemistry, Physical and Theoretical Chemistry Laboratory, University of Oxford, South Parks Road, Oxford, OX1 3QZ, United Kingdom.
b. Semiconductor & Energy Conversion - Center for Electrochemical Sciences (CES), Ruhr-Universität Bochum, 44780 Bochum, Germany.
c. Analytical Chemistry - Center for Electrochemical Sciences (CES), Ruhr-Universität Bochum, 44780 Bochum, Germany.
d. Catalonia Institut for Energy Research (IREC), Jardins de les Dones de Negre, 08930 Sant Adrià de Besòs, Barcelona, Spain
e. Universität Bremen, Energiespeicher- und Energiewandlersysteme, 28359 Bremen, Germany.

This electronic supporting information contains 5 sections:

Section 1: Materials synthesis

Section 2: XRD characterisation

Section 3: Analysis of the electrochemical stability of the Fc^+/Fc redox couple.

Section 4: Electrochemical properties of a porous $LiNi_{0.5}Mn_{1.5}O_4$-based paste electrode surface through SECM area mapping.

1. Materials Synthesis

$LiNi_{0.5}Mn_{1.5}O_4$ was synthesized following a previously reported porous polymer precursor method [1]: 1.5 g of cosmetic cotton swabs obtained from a local drug store were soaked in 50 ml of three solutions formed by 0.0105 M $LiNO_3$, 0.15 M $Mn(NO_3)_2 \cdot H_2O$, and 0.05 M $Ni(NO_3)_2 \cdot 6H_2O$ (Sigma-Aldrich) for 3 hours. They were then squeezed in order to remove the liquid in excess. The damp cotton was therefore placed in a box furnace and heated in air at a rate of 100 °C per hour until reaching a temperature of 400 °C. To obtain the final powders, the carbonized cotton was collected, grinded and calcined at 800 °C for 4 h in air.

$Li_{1+x}(Ni_{1/3}Mn_{1/3}Co_{1/3})_{1-x}O_2$ either stoichiometric (x=0) or overlithiated (x=0.1) were prepared following a slightly modified method as proposed by K. Zaghib et al.[2]: nickel, cobalt and manganese oxalate $(Ni_{1/3}Co_{1/3}Mn_{1/3})C_2O_4$ precursors were synthesized through a co-precipitation method using an aqueous solution of $Ni(NO_3)_2 \cdot 6H_2O$, $Co(NO_3)_2 \cdot 6H_2O$ and $Mn(NO_3)_2 \cdot 4H_2O$ (cationic ratio of Ni/Co/Mn = 1:1:1), in which 100 mL of oxalic acid with a concentration of 1 M was drowsily added by stirring, until complete precipitation of the oxalate precursor. The product was filtered, and then dried at 100 °C for 12 h. Afterwards, the desired amount of lithium hydroxide was mixed thoroughly with the dried powder and annealed at 480 °C for 4 h in air to obtain $Li(Ni_{1/3}Mn_{1/3}Co_{1/3})O_2$ or $Li_{1.1}(Ni_{1/3}Mn_{1/3}Co_{1/3})_{0.9}O_2$. The material was grinded and calcined at 900 °C for 6 h in air in order to obtain the final powders.

2. XRD Characterisation

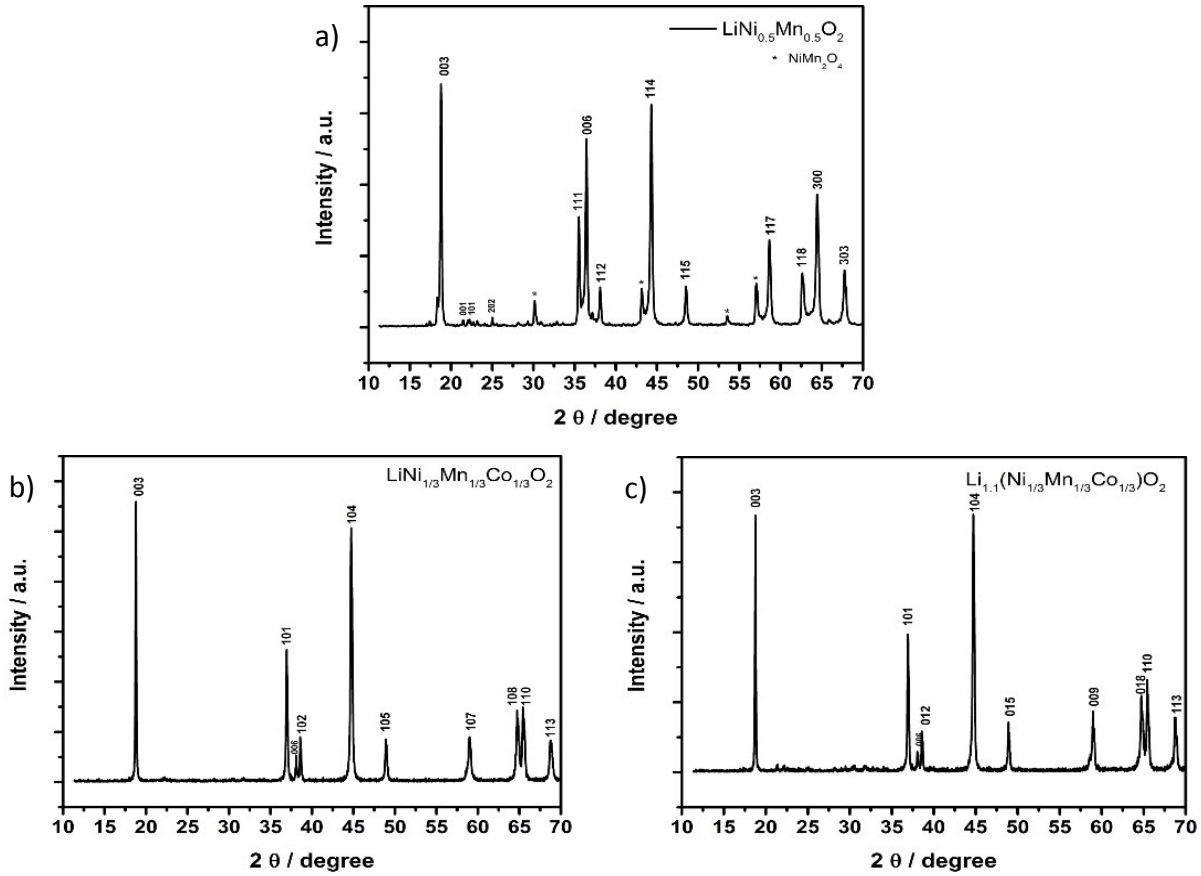

Figure SI 1. XRD pattern of pristine a) $LiNi_{0.5}Mn_{0.5}O_2$, b) stoichiometric $LiNi_{1/3}Mn_{1/33}Co_{1/3}O_2$ and c) overlithiated $Li_{1.1}Ni_{1/3}Mn_{1/33}Co_{1/3}O_2$.

All synthesized lithium oxides powders were analyzed by X-ray diffraction (figure SI 1). Their lattice parameters are in agreement with the ones previously reported [3-6]. The narrow peaks indicate a high crystallinity. Unlike $LiNi_{0.5}Mn_{1.5}O_4$, where classic $NiMn_2O_4$ impurities were found, there was not any evidence of impurities for the $LiNi_{1/3}Mn_{1/33}Co_{1/3}O_2$ and $Li_{1.1}Ni_{1/3}Mn_{1/33}Co_{1/3}O_2$ samples.

3. Analysis of the electrochemical stability of the Fc^+/Fc redox couple

Cyclic voltammograms of two fresh Pt microelectrodes (radius 12.5 µm) recorded in the bulk of the solution, are shown in presence and in absence of ferrocenium ions (Fc^+) (figure SI 2). In absence of Fc^+ (red line) an oxidation process involving the electrolyte components can be seen starting from a potential of circa 4.6 V vs. Li/Li^+. When Fc^+ is present in solution (black line), an irreversible peak appears at circa 4.4 V vs. Li/Li^+, suggesting that the Fc^+ undergoes an irreversible oxidation process in agreement with ref.[7].

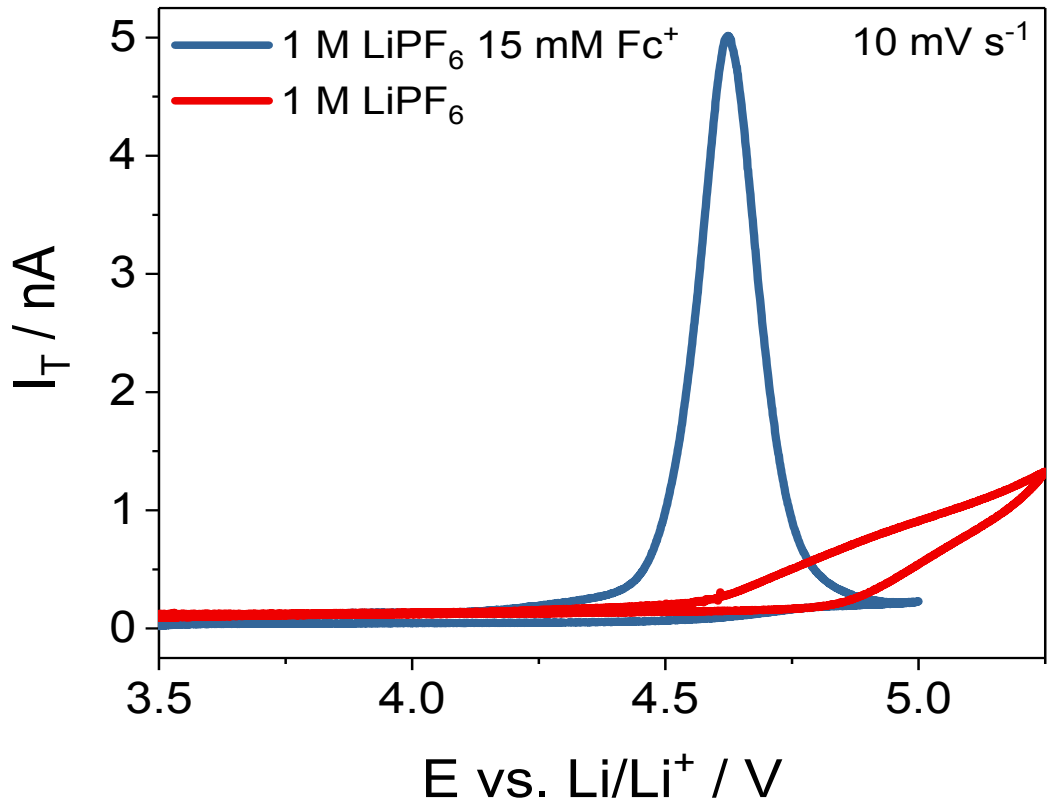

Figure SI 2: Cyclic voltammogram of a Pt microelectrode in 1 M $LiPF_6$ EC:DEC (1:1 wt.%) (red line) containing 15 mM ferrocenium hexafluorophosphate (black line).

This phenomenon was found to affect also the electrochemical behavior of all lithium oxides analyzed in the frame of this work. For example, figure SI 3 shows the voltammograms of two fresh $LiNi_{0.5}Mn_{1.5}O_4$ based paste electrodes cycled between 4 V and 5.2 V vs. Li/Li^+ in presence and in absence of ferrocenium hexafluorophosphate.

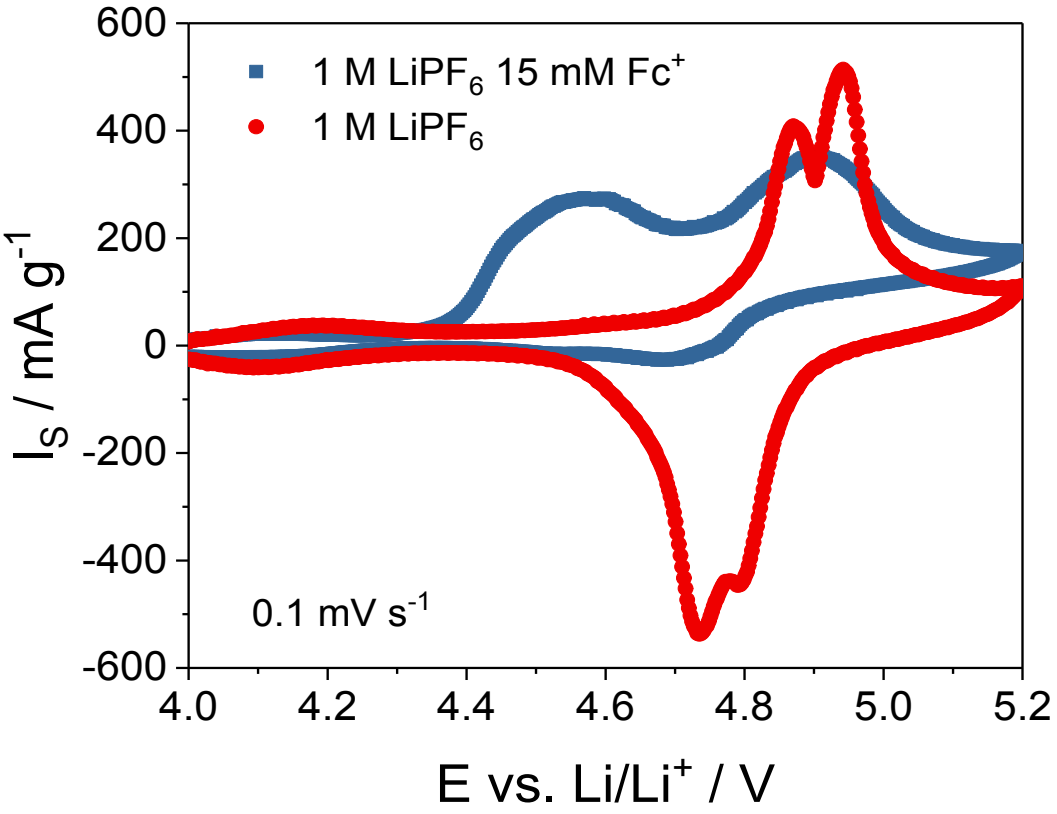

Figure SI 3: C yclic voltammogram of $LiNi_{0.5}Mn_{1.5}O_4$-based paste electrode in 1 M $LiPF_6$ EC:DEC (1:1 wt.%) (red line) containing 15 mM ferrocenium hexafluorophosphate (black line).

The two voltammograms show a very different shape. In absence of Fc^+ the two-stages deinsertion of Li^+ takes place in a potential range between 4.8 V and 5 V vs. Li/Li^+, while the subsequent two-stages Li^+ insertion occurs between 4.9 V and 4.7 V vs. Li/Li^+, as expected. On the contrary, when Fc^+ is present in the electrolytic solution, a broad peak appears at 4.4 V vs. Li/Li^+ in the anodic branch of the voltammogram, followed by another broad peak at 4.9 V vs. Li/Li^+. This can be ascribed to the poor stability of the Fc^+ at high anodic potentials, but also to a strong interaction of the redox mediator with the (de-)insertion processes of Li^+ into the mixed oxide structure. Because of the instability of the redox couple plus its detrimental interactions with the active materials, only an *in-situ* and not *in-operando* (i.e. while polarizing the electrode under investigation) analysis of the electronic character of all the paste electrodes and Al current collector surface could be performed.

4. Electrochemical properties of a porous $LiNi_{0.5}Mn_{1.5}O_4$-based paste electrode surface through SECM area mapping

In figure SI 4 the area scan of a 250 × 250 µm² region of a $LiNi_{0.5}Mn_{1.5}O_4$-based paste electrode cycled once from OCP to 5.25 V vs. Li/Li+ is shown. The Pt microelectrode (SECM tip) was approached to the sample surface at a distance of 15 µm through the piezo system belonging to the SECM apparatus. The tip-to-sample distance was kept constant throughout the overall area scan thanks to a feedback loop controller.

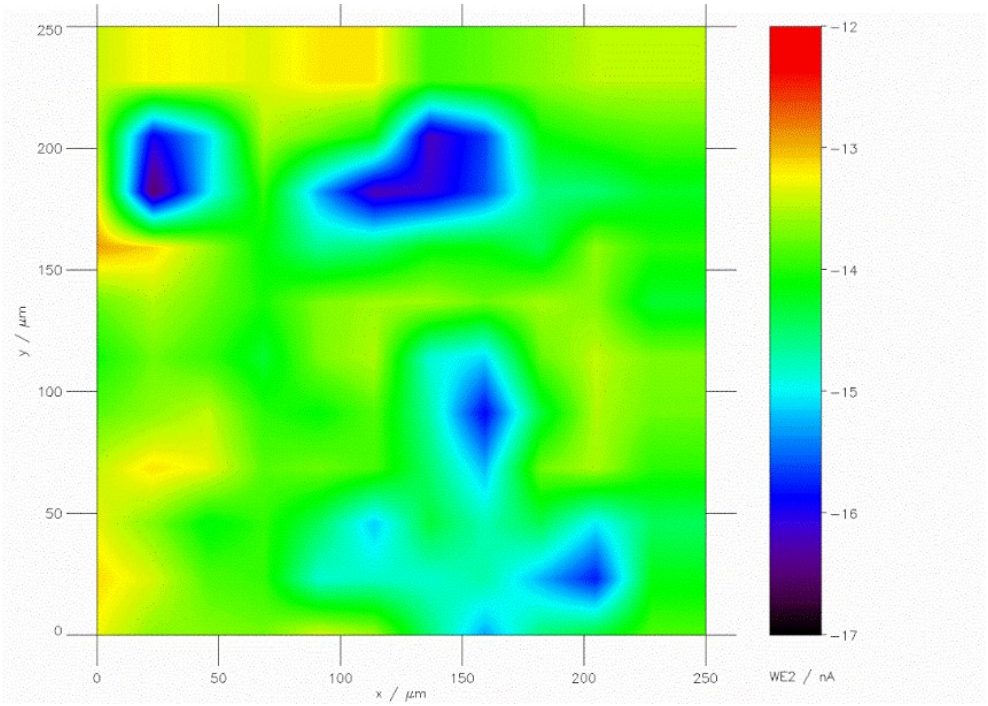

Figure SI 4: SECM area mapping of a $LiNi_{0.5}Mn_{1.5}O_4$-based paste electrode cycled once from OCP to 5.25 V vs. Li/Li^+ in 1 M $LiPF_6$ in EC:DEC (1:1 wt.%) at a scanrate of 0.1 mV s^{-1}. The area mapping was recorded in a solution containing 15 mM Fc^+ and 1 M $LiPF_6$ in EC:DEC (1:1 wt.%). Applied potential at the Pt tip: 3.0 V vs. Li/Li^+. Applied potential at the $LiNi_{0.5}Mn_{1.5}O_4$-based paste electrode: 4.1 V vs. Li/Li^+.

Both the active material particles and the carbon additive have dimensions below 1 µm, and they are thus too small to be resolved by the Pt SECM tip whose radius is 12.5 µm. Therefore, the features shown in the area scan have to be ascribed to the topography variations of the porous paste electrode surface. Hence, it can be concluded that the data collected from a single point z-approach curves for the in-situ analysis of the electronic character of the active materials are representative for the average behavior of the sample surface. The same conclusion can be drawn in the case of the other paste electrodes, since also in those cases the average dimension of the active material particles was around 1 µm.

In Fig SI 5 the z-approach curves recorded after the area mapping of the same LMN paste electrode in four different grid points are shown. The spatial coordinate reported is the relative Z-axis of the SECM positioning system. As it can be seen, the point of maximum approach is located at a normalized current value of c.a. 2.3 (which would correspond to a cathodic current of the Fc^+ reduction of c.a. -28 nA) for all cases. The fact that in each point the current of maximum approach has almost the same value indicates that a single point is representative of the reactivity of the whole surface. Moreover the fact that the point of maximum approach is reached ad different z values, is a further indication of the topographical variation of the porous electrode.

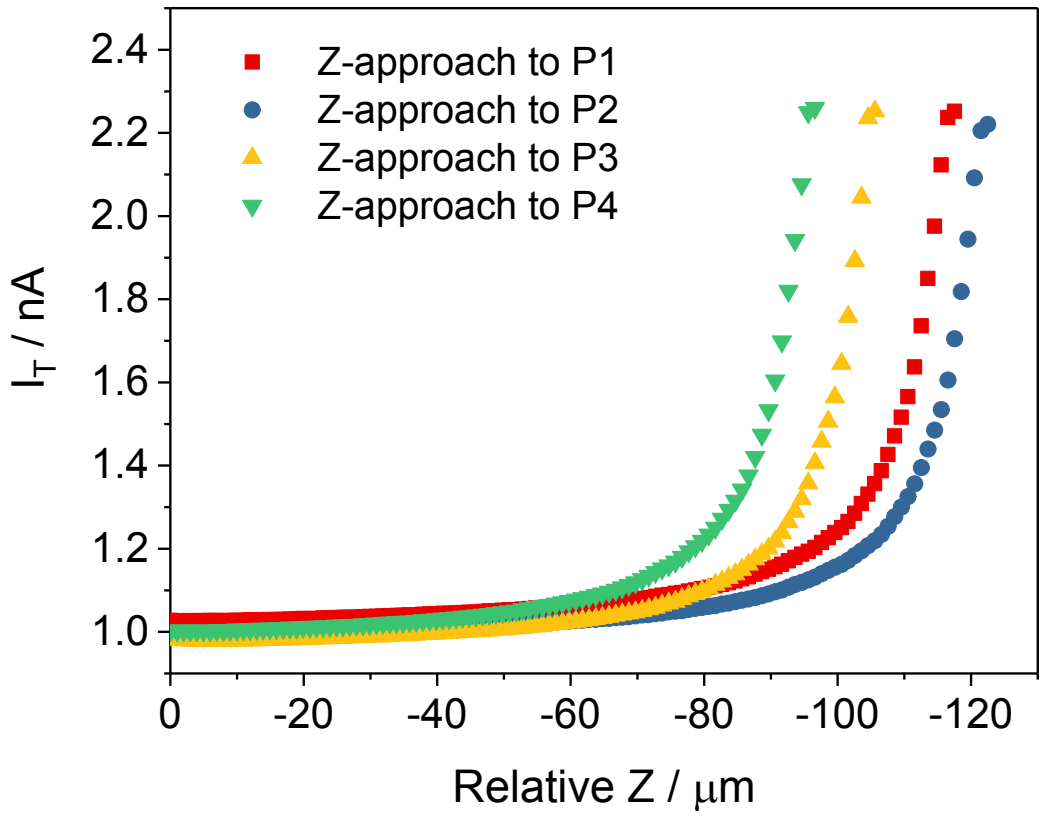

Figure SI 5: SECM Z-approach curves towards a $LiNi_{0.5}Mn_{1.5}O_4$-based paste electrode cycled once from OCP to 5.25 V vs. Li/Li^+ in 1 M $LiPF_6$ in EC:DEC (1:1 wt.%) at a scanrate of 0.1 mV s^{-1}. All the Z-approach curves were recorded in a solution containing 15 mM Fc^+ and 1 M $LiPF_6$ in EC:DEC (1:1 wt.%). Applied potential at the Pt tip: 3.0 V vs. Li/Li^+. Applied potential at the $LiNi_{0.5}Mn_{1.5}O_4$-based paste electrode: 4.1 V vs. Li/Li^+.

References

1. H. D. Deshalzer, F. La Mantia, C. Wessels, R. A. Huggins, Y. Cui, *J. Electrochem. Soc.*, 2011, **158**, A1079;
2. A. M. A. Hashem, A. E. Abdel-Ghany, A. E. Eid, J. Trottier, K. Zaghib, A. Mauger, C. M. Julien, *J. Power Sources*, 2011, **196,** 8632;
3. Y. S. Meng, G. Ceder, C. P. Grey, W. S. Yoon, Y. Shao Horn, *Electrochem. Solid-State Lett.,* 2004, **7,** A155;
4. D. Wang, I. Belharouak, G. Zhou, K. Amine, *Adv. Funct. Mater.,*2013, **23,** 1070;
5. X. Liao, Q. Huang, S. Mai, X. Wang, M. Xu, L. Xing, Y. Liao, W. Li, *J. Power Sources*, 2015, **286,** 551;
6. F. Rosciano, J.F. Colin, F. La Mantia, N. Tran, P. Novák, *Electrochem. Solid-State Lett.*, 2009, **12**, A140;
7. M. N. Golovin, D. P. Wilkinson, J. T. Dudley, D. Holonko, S. Woo, *J. Electrochem. Soc.*, 1992, **139**, 5;